PERGAMON

International Journal of Heat and Mass Transfer 43 (2000) 1801–1809

International Journal of HEAT and MASS TRANSFER

www.elsevier.com/locate/ijhmt

Radiative heat transfer in natural gas-fired furnaces

E.P. Keramida[a], H.H. Liakos[a], M.A. Founti[b], A.G. Boudouvis[a], N.C. Markatos[a,*]

[a]*Department of Chemical Engineering, National Technical University of Athens, Zografou Campus, Athens 157 80, Greece*
[b]*Department of Mechanical Engineering, National Technical University of Athens, Zografou Campus, Athens 157 80 Greece*

Received 8 April 1999; received in revised form 26 July 1999

Abstract

The performance of the discrete transfer and of the six-flux radiation models is assessed in a swirling natural gas diffusion flame confined in an axisymmetric furnace. The predictions are evaluated as part of a complete prediction procedure involving the modeling of the simultaneously occurring flow, combustion, convection and radiation phenomena. Computational results with and without radiation effects are compared with experimental data and the two radiation models are evaluated in terms of computational efficiency, ease of application and predictive accuracy. The results have demonstrated that the effect of thermal radiation is important even in light flames, and that the six-flux model can be applied in industrial gas furnaces with relative ease, yielding accurate predictions.

Keywords: Radiation; Natural gas furnaces; Six-flux model; Discrete transfer model

1. Introduction

Thermal radiation in gaseous media can be an important mode of heat transfer in high temperature chambers, such as industrial furnaces and boilers, even under non-soot conditions. Growing concern with high temperature processes has emphasized the need for an evaluation of the effect of radiative heat transfer. For example, thermal radiation affects significantly the structure and extinction characteristics of a methane–air flame due to the radiative cooling mechanism [1,2], as well as the NO formation due to the sensitivity of thermal NO kinetics to temperature [3].

Nevertheless, the modeling of radiative transfer is often neglected in combustion analysis, mainly because it involves complex mathematics, high computational cost, and significant uncertainty concerning the optical properties of the participating media and surfaces. However, ignoring radiative transfer may introduce significant errors in the overall predictions.

In previously published evaluations of radiation models for gaseous furnaces, the models are tested separately, that is, in isolation from other physical processes, by using prescribed radiative energy source term distributions [4–10]. In real operating furnaces though, non-uniform distributions of velocity and temperature are encountered and the predictive behavior of any radiation model is expected to differ from the simplified case [4,11].

A numerical experiment is carried out in this paper, using two different radiation models to analyze the radiative heat transfer in an industrial natural-gas furnace configuration. The predictions are evaluated as

* Corresponding author. Tel.: +30-1-772-3227; fax: +30-1-772-3228.
E-mail address: ellik@chemeng.ntua.gr (N.C. Markatos).

0017-9310/00/$ - see front matter
PII: S0017-9310(99)00244-6

Nomenclature

C_A	reaction rate constant
C_R	reaction rate parameter
E	emissive power [W m^{-2}]
e_w	surface emissivity
I	radiative intensity [W m^{-2}]
J	mean intensity of the in-scattered radiation [W m^{-2}]
k_a	gas absorption coefficient [m^{-1}]
k_s	gas scattering coefficient [m^{-1}]
k	turbulence kinetic energy [m^2 s^{-2}]
L	path length [m]
m	mass fraction
Q	total attenuation of the radiative intensity due to emission and in-scattering [W m^{-2}]
$\bar{R}$	reaction rate [kg m^{-3} s^{-1}]
R	radiation flux [W m^{-2}]
$\mathbf{r}$	direction vector
S	stoichiometric value
S_Φ	source term
S_{rad}	radiative energy boundary source term [W m^{-2}]
$\mathbf{s}$	location vector
T	temperature [K]
t	time [s]
x, r	co-ordinate axes in cylindrical geometry
$\mathbf{u}$	velocity vector [m s^{-1}]

Greek symbols

Γ_Φ	diffusion coefficient
ε	dissipation of energy [m^2 s^{-3}]
κ	extinction coefficient [m^{-1}]
μ	viscosity [kg m^{-1} s^{-1}]
ρ	density [kg m^{-3}]
σ	Stefan–Boltzmann constant, 5.67×10^{-8} [W m^{-2} K^{-4}]
τ	optical thickness
Φ	transport variable
Ω	solid angle

Subscripts

f	fuel
n	zone number
o	oxygen
p	products
r	radial direction
w	wall
x	axial direction

part of a complete prediction procedure involving the modeling of the simultaneously occurring flow, combustion, convection and radiation phenomena.

1.1. Radiation modeling

There are several analytical methods presently used for the engineering treatment of radiative heat transfer in participating media. The most accurate ones are considered to be the zone [12] and the Monte Carlo [13] methods. However, these methods are not widely used in comprehensive combustion calculations due to their large computational time and storage requirements. Additionally, the above-mentioned models are in non-differential form, providing a significant inconvenience in solving them simultaneously with the remaining equations of fluid flow.

For industrial furnace applications, radiation modeling is directed towards more efficient but less fundamental flux methods (see [14] for an extensive review). Modeling of the simultaneously occurring flow, chemical reaction, and heat transfer in a transient furnace atmosphere involving more than one phases, can be a CPU demanding procedure. As efficiency is particularly important in the development of furnace simulation codes, the radiation model used should not only be realistic enough to yield meaningful predictions, but also simple and fast enough to avoid overcharging the computational cost.

One such model is the six-flux model of Schuster and Hamaker, as formulated by Spalding (see [15] for a detailed description). Easy to understand, readily applicable and fast, but of limited accuracy, has successfully been applied to a number of furnace cases. On the other hand, the discrete transfer model of Lockwood and Shah [6], has received much attention in the engineering treatment of furnace radiation, during the last decade; combining features of the zone, Monte Carlo and the flux models, is considered as a more fundamental and accurate model.

These two models are applied here to a benchmark natural gas furnace case, attempting to evaluate them in terms of computational efficiency, ease of application and predictive accuracy. The strengths and limitations of the two models are discussed below.

With the discrete transfer model, the total radiative flux is calculated by integrating the energy contribution along rays emanating from the radiative source and

pointing to any selected direction. The discrete transfer model has the following advantages and disadvantages:

advantages

— retains the physics of the problem with relatively simple mathematics;

— has the ability to return any desired degree of accuracy by increasing the number of rays projected from each physical surface and the number of zones that the domain is divided into, adding of course considerably to the cost of computation;

disadvantages

— requires a surface model to describe the geometry;

— requires carefully shaped control volumes and positioning of the rays to yield accurate predictions.

The six-flux method accounts for contributions to the radiative flux coming from only six directions, parallel and anti-parallel to the three coordinate directions. It is a differential model providing convenience in the discretisation of the transport equations. The six-flux model has the following advantages and disadvantages:

advantages

— retains the important effects relevant to furnace scenarios, although it assumes that radiation is transmitted in coordinate directions only;

— offers computational economy;

— solves directly on the flow spatial grid, needs no special description of the geometry;

disadvantages

—has no inter-linkages, apart from scattering, between the radiation fluxes in the respective coordinate directions;

— is quite accurate for optically thick media, but it will yield inaccurate results for thinner (transparent) media, especially near boundaries, and also if the radiation field is anisotropic;

— fails in cases of complex geometry, such as congested spaces, or many and large openings.

2. The physical and mathematical model

2.1. Furnace configuration

The benchmark case studied is a typical chamber of gaseous combustion, the so-called "Harwell furnace', which is a cylindrical enclosure of 0.15 m radius and 0.9 m length [16,17]. Two reactant streams emerge from two separate coaxial jets producing a swirling diffusion flame. The fuel is injected from the central jet

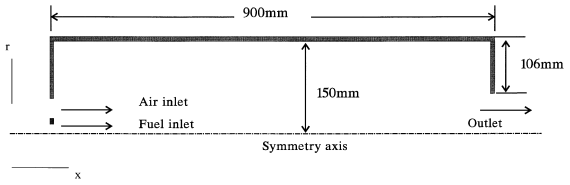

Fig. 1. Geometry of the combustion chamber.

whereas the combustion air enters from the outer annular jet. The geometry of this natural gas furnace is illustrated in Fig. 1 and the inlet conditions for the fuel and air are shown in Table 1.

2.2. Mathematical model

A two-dimensional mathematical model is used to simulate the flow and chemical reaction in the combustion chamber. The model consists of the partial differential equations describing the conservation of momentum, heat and mass, in conjunction with a two-equation turbulence model. The equations are expressed, for each variable, in a generalized form as:

$$\frac{\partial}{\partial t}(\rho\Phi) + \mathrm{div}(\rho\mathbf{u}\Phi - \Gamma_\Phi \,\mathrm{grad}\,\Phi) = S_\Phi \tag{1}$$

where Φ is any of n variables [18], Γ_Φ is the diffusion coefficient and S_Φ is the source term of the variable Φ. The turbulence kinetic energy and the dissipation of turbulence are calculated with the k–ε model [19].

The heat release of methane/air combustion is calculated by the eddy dissipation model [20], considering an integral, fast, one-step reaction $CH_4 + 2O_2 \leftrightarrow$

Table 1
Input conditions and fluid properties

Geometry		
Fuel inlet zone (mm)	from r = 0.0	to r = 6.0
Air inlet zone (mm)	from r = 16.5	to r = 27.5
Furnace diameter (mm)	150.0	
Furnace length (mm)	900.0	
Inlet boundary conditions	*Fuel*	*Air*
Axial velocity	15.0	12.8
Radial velocity	0.0	0.0
Turbulent kinetic energy	2.26	1.63
Dissipation rate of turbulence	1131.8	692.0
Temperature	295	295
Swirl number	0.0	0.4
Composition (mass fraction)	*Fuel*	*Air*
O_2	0.0	0.2315
N_2	0.0	0.7685
CH_4	1.0	0.0
Heat of reaction (MJ/kg)	45.5	

$CO_2 + 2H_2O$. This solves for one combustion scalar variable, the mean mixture fraction and the mass fraction of the fuel. In each computational cell, the reaction rate is set as:

$$\bar{R} = C_A C_R \rho \frac{\varepsilon}{k} \min\left(m_f, \frac{m_o}{S}, \frac{m_p}{1+S}\right) \tag{2}$$

where

$$C_R = 23.6\left(\frac{\mu\varepsilon}{\rho k^2}\right)^{1/4} \tag{3}$$

and C_A is an empirical constant taken equal to 1 [20], μ is the gas viscosity, ρ is the gas density, ε is the turbulence dissipation, k is the turbulence kinetic energy, m_f, m_o, m_p, are the mass fractions of the fuel, oxygen and products, respectively, and S is the stoichiometric value taken equal to 17.189.

The combustion gas is taken as a mixture of oxygen, nitrogen, carbon dioxide, water vapor and fuel gas. The gas temperature is derived from the enthalpy equation where the specific heat is calculated as the weighted sum of the individual specific heat of the mixture components. The gas density is evaluated from the ideal gas equation of state. All computations are conducted by using a finite volume discretisation scheme.

2.3. Radiation models

The basis of all methods for the solution of radiation problems is the radiative transfer equation (RTE):

$$\mathbf{s}\cdot\nabla I(\mathbf{r},\mathbf{s}) = -\kappa(\mathbf{r})I(\mathbf{r},\mathbf{s}) + Q(\mathbf{r},\mathbf{s}) \tag{4}$$

which describes the radiative intensity field, I, within the enclosure, as a function of location vector $\mathbf{r}$ and direction vector $\mathbf{s}$; Q represents the total attenuation of the radiative intensity due to the gas emission and to the in-scattered energy from other directions to the direction of propagation, and κ is the total extinction coefficient.

2.4. The discrete transfer model

The discrete transfer model discretizes the RTE along rays. The path along a ray is discretized by using the sections formed from breaking the path at zone boundaries. Assuming that the physical properties remain constant inside a zone, Eq. (4) can be integrated from zone entry to zone exit (Fig. 2) to yield:

$$I_{n+1} = I_n e^{-\tau_n} + L_n Q_n\left[\frac{1-e^{\tau_n}}{\tau_n}\right]; \tau_n = \kappa L_n \tag{5}$$

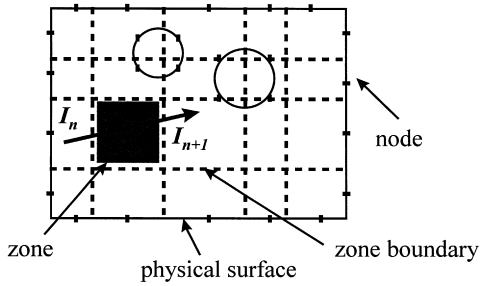

Fig. 2. Sub-division of the solution domain into zones.

where L_n is the path length in the nth zone, I_n and I_{n+1} are the intensities at zone entry and zone exit respectively, and

$$Q_n(\mathbf{r},\mathbf{s}) = \frac{k_a}{\pi}\sigma T_n^4 + k_s J_n(\mathbf{r}) \tag{6}$$

where k_a, k_s, are the absorption and scattering coefficients for a gray medium, $J_n(\mathbf{r}) = \frac{1}{4\pi}\int I_n(\mathbf{r},\mathbf{s})\,d\Omega$ is the mean intensity of the in-scattered radiation, σ is the Stefan–Boltzmann constant and $d\Omega$ is the element of solid angle containing $\mathbf{s}$.

The rays are chosen by fixing nodes to all the physical surfaces, dividing up the interior hemi-sphere into elements of equal solid angle and projecting one ray into each solid angle.

For gray surfaces, integration of Eq. (4) yields the required boundary conditions:

$$I(\mathbf{r},\mathbf{s}) = \frac{e_w}{\pi}\sigma T^4(\mathbf{r}) + \frac{1-e_w}{\pi}R(\mathbf{r}) \tag{7}$$

where e_w is the wall emissivity, and $R(\mathbf{r}) = \int_{\mathbf{s}\cdot\mathbf{n}<0}(\mathbf{s}\cdot\mathbf{n})I(\mathbf{r},\mathbf{s})\,d\Omega$ is the radiation flux on a surface, and $\mathbf{n}$ is the inward pointing unit vector normal to the surface at $\mathbf{r}$.

2.5. The six-flux model

The model employs diffusion-type differential equations for calculating radiative heat transfer. The solid angle surrounding a point is divided into six solid angles. The following second-order ordinary differential equations describe in polar coordinates the six-flux model, for a two-dimensional case (actually a four-flux):

$$\frac{1}{r}\frac{d}{dr}\left[\frac{1}{k_a+k_s+\frac{1}{r}}\frac{d(R_r)}{dr}\right] = R_r(k_a+k_s) - k_a E - \frac{k_s}{2}(R_r+R_x) \tag{8}$$

$$\frac{\mathrm{d}}{\mathrm{d}x}\left[\frac{1}{k_a+k_s}\frac{\mathrm{d}(R_x)}{\mathrm{d}x}\right]$$

$$= R_x(k_a+k_s) - k_aE - \frac{k_s}{2}(R_r+R_x) \quad (9)$$

R_r, R_x are the composite radiative fluxes in radial and axial directions respectively. Each of the differential flux equations expresses the attenuation of a flux with distance as a result of absorption and scattering and its augmentation by emission and scattering from other directions.

The required boundary source term, S_{rad}, for a wall is:

$$S_{rad} = \frac{e_w}{2-e_w}(E_w - R_w) \quad (10)$$

where $E_w = \sigma T_w^4$, is the emissive power on the wall, e_w is the emissivity constant on the wall and R_w is the radiation flux near the wall.

At symmetry planes and perfectly-reflecting boundaries, the radiative heat flux is zero. At non-reflecting boundaries, such as openings or free boundaries, the outgoing radiation leaves the computational domain without reflection.

3. Computational details

As already mentioned, the discrete transfer model may yield any desired degree of precision by increasing the number of rays and the number of zones. Results with various numbers of rays have been obtained, and these demonstrate that 32 rays suffice for accurate predictions.

Absorption and scattering coefficients used in the radiation model are taken 0.5 m^{-1} and 0.01 m^{-1}, respectively [16]. The walls are treated as a gray heat sink of emissivity 0.8 and assumed to be completely water-cooled at a temperature of 400 K [16]. The CPU time consumed on an SGI Workstation R4400 are 530 min for the six-flux model and 805 min for the discrete transfer model.

4. Results

Comparisons between the experimental data reported by Wilkes et al. [16] and the calculated results obtained with and without radiation are shown in Figs. 3–5. The variation of temperature along the furnace centerline is presented in Fig. 3. In Fig. 4, radial profiles of the temperature are shown for four consecutive axial locations; two near the inlets and two near the middle of the furnace. It is shown that accounting for radiation in the computational analysis, by any of the two methods, has produced better agreement between the predictions and the experimental data.

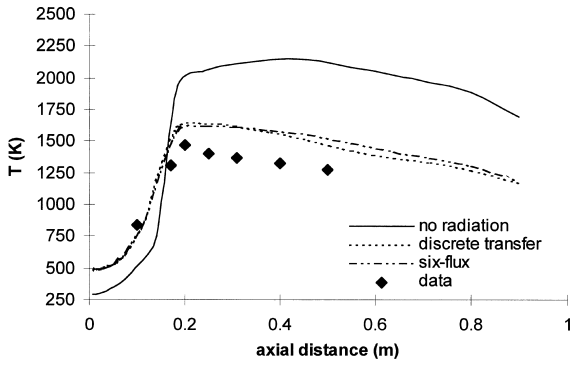

Fig. 3. The variation of temperature along the furnace centerline.

The reduction of the mean temperature in the furnace is significant, and is more pronounced in the upstream direction, towards the furnace outlet. Close to the furnace inlets, on the other hand, an increase in temperature is predicted. This shows that the reactant mixture heating effect, due to the flame backward radiation, is better represented when radiative heat transfer is taken into account (see Fig. 3). Similar observations can be made from the radial temperature profiles shown in Fig. 4, at $x = 0.04$ m and $x = 0.1$ m. In the main combustion zone, where higher temperatures are reached, the effects of radiation are more evident and extend all over the furnace diameter (see Fig. 4, radial profiles at $x = 0.2$ m and $x = 0.4$ m). No significant differences are observed between the predicted temperatures with the two radiation models.

Despite the fact that the overall heat released is the same in all the examined cases, radiative heat transfer is responsible for reducing the size of the high temperature regions of the flame and for shifting them towards the furnace inlet, as it is shown by the temperature contours in Fig. 5. As a result, more heat is released close to the burner when radiation is taken into account, resulting to steeper temperature gradients towards the furnace outlet. The combustion gases leave the furnace with nearly 60% lower temperature. This reduction of the gas enthalpy content at the outlet is counter-balanced by the increase of the total heat flux across the axial wall of the furnace; the total heat loss from the wall is increased by four times.

Fig. 6 shows the variation of the heat flux along the furnace axial wall. Absolute wall heat flux values are significantly increased when radiation is taken into account. The main combustion zone temperatures, around the central part of the furnace do not seem to directly affect the heat losses from the

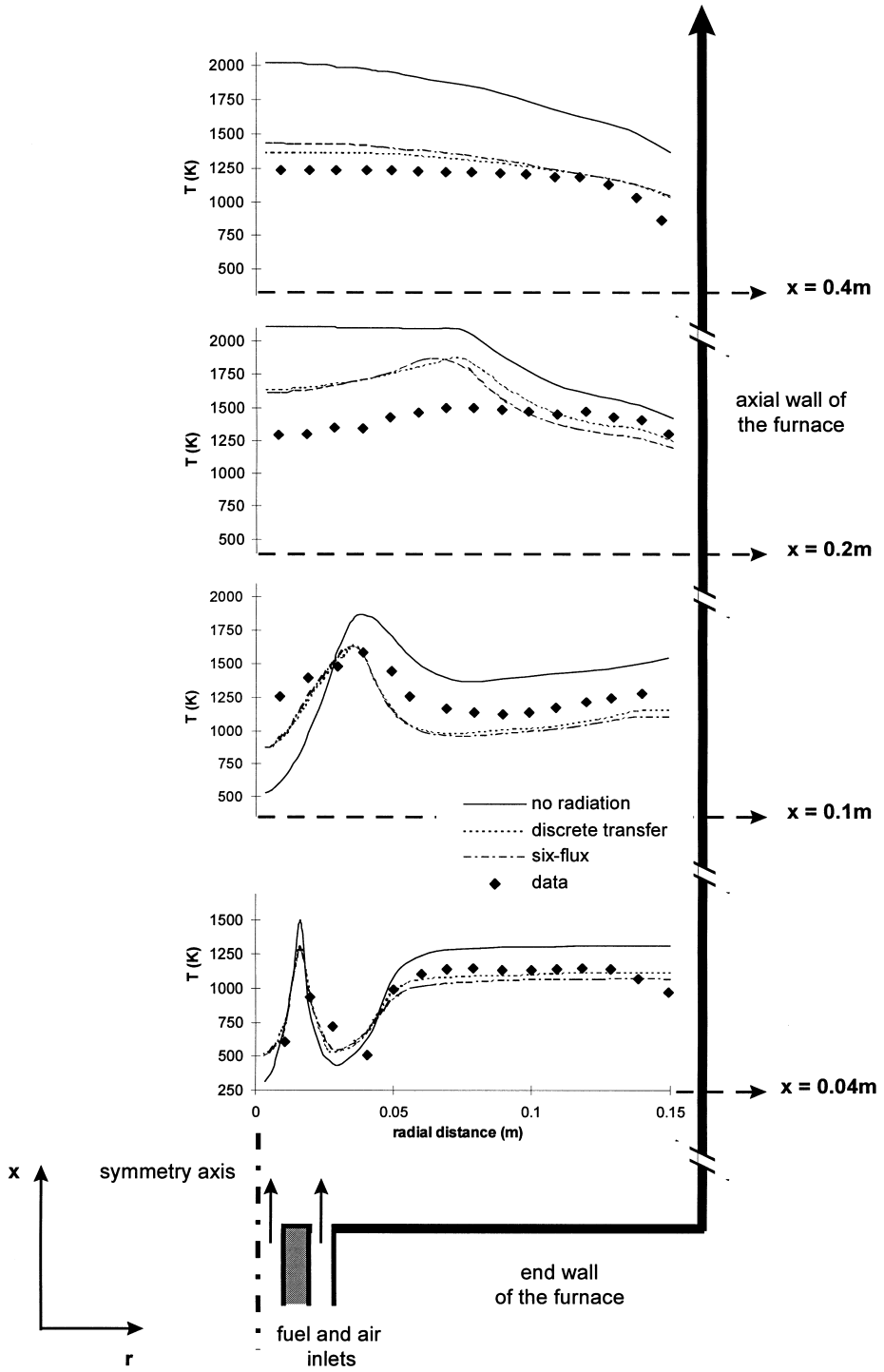

Fig. 4. Radial temperature profiles at distances 0.04, 0.1, 0.2 and 0.4 m from entrance.

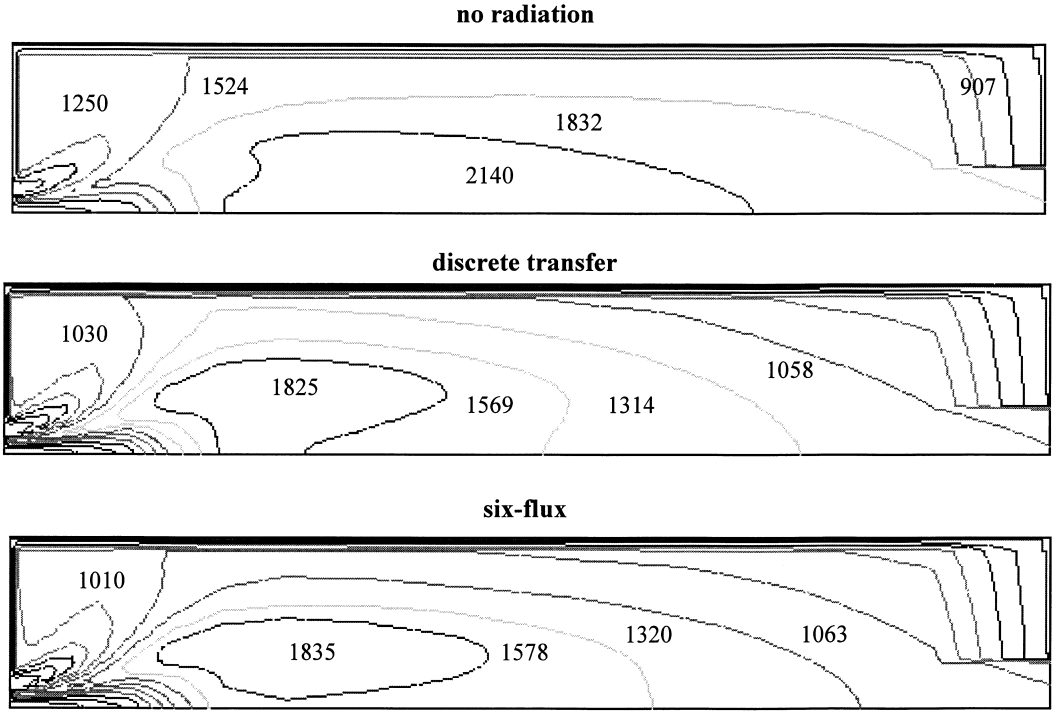

Fig. 5. Contours of constant temperature.

wall. When radiation is taken into account, the total heat flux from the furnace wall is due to the sum of contributions of the convective and radiative heat transfer. The axial location of the maximum wall heat-flux value is shifted downstream, where maximum temperatures are encountered in the main combustion zone of the furnace. The total heat leaving through the axial wall of the system has increased about four times.

Finally, in terms of predictive accuracy, the two radiation models have performed similarly. This can be explained by the fact that there is a relative uniformity in the combustion gases concentration field encountered in a natural gas-fired furnace, and radiation is isotropic. These characteristics of the medium are fairly represented by the applied constant optical properties. If the system is highly non-uniform, featuring many and large areas of optical thinness (e.g. a fire environment [21]), then the six-flux model will do poorly. The reason is that in the absence of absorption and scattering the transport equations describing the six-flux model will 'transmit' radiation from z_1 to z_2 etc., but not from z_1 to y_1 (see Fig. 7), hence producing erroneous results. In practice this means that the z wall will only 'feel' the radiation from the y wall via absorption and scattering within the gas. In the case under consideration, the medium is semi-transparent, with a relatively medium opacity, obscuring this par-

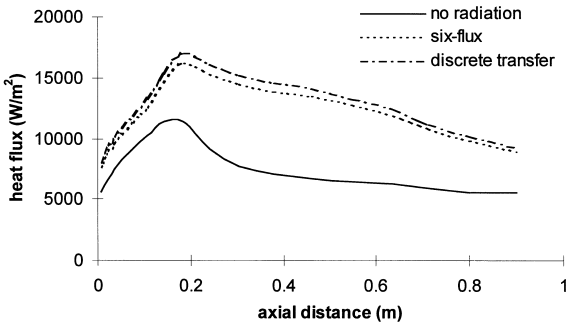

Fig. 6. Heat flux distribution along the axial furnace wall.

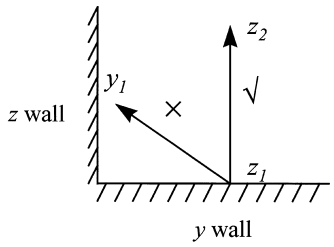

Fig. 7. Radiation transfer as described by the six-flux model, for the case of a transparent gas.

ticular weakness of the six-flux model. In any other case, where transparent areas are involved the above described limitation of the six-flux model will be more pronounced.

The fact that the two radiation models have performed similarly, confirms that the six-flux model, although crude in principle, is adequate for predicting the overall features of the flow, in light natural gas furnaces. This is an important result when it comes to simplified heat transfer analysis in combustion simulations, given that the six-flux model is significantly simpler than the discrete transfer model, regarding mathematics and implementation effort. It should be noted that this model offers a significant convenience for the engineer, that it can easily be incorporated in any 2-D CFD analysis by simply introducing two scalar transport equations into the calculations — describing the diffusive transfer of the radiation fluxes — and by setting the corresponding boundary conditions.

Concerning the implementation effort for the discrete transfer model, this is related to the fact that the model requires a geometrical description of its own to work. The construction of the geometry, which is based on surface modeling, requires carefully selected control volumes (zones) and positioning of the rays to achieve the required solution. The results produced by the discrete transfer model are sensitive to the zone construction. Crude or careless 'zoning' of the heat source (flame) result in inaccurate average values of the temperature per zone and, consequently, to inaccurate radiation calculations. The reason for that is that in large systems the spatial resolution (number of zones) is normally much less than that used by the flow solver. This mainly affects the cooling rate, which is proportional to the fourth power of the temperature and thus it can change by several orders of magnitude across a flame front. Large local errors occur, if large opacity gradients remain unresolved by the radiation model. In Fig. 8, case 1 is an example of crude zoning, while case 3 is an example of more careful zoning that takes into account the steep temperature variation from zone to zone. Another important issue when 'zoning' the heat sources, is to ensure symmetry; comparison between case 2a and case 2b in Fig. 8 shows the difference.

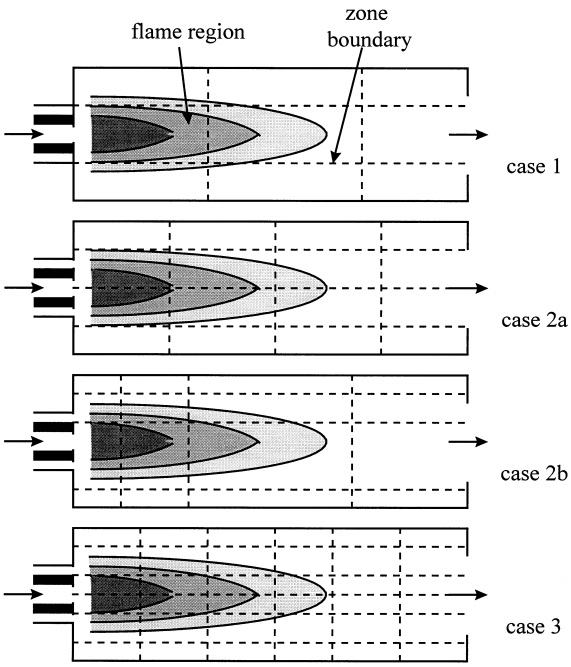

Fig. 8. Hypothetical zone constructions, showing different sampling of the flame.

5. Conclusions

There is difference between evaluating radiation models as part of an overall predictive scheme and evaluating them independently, as the coupled effects of different interplaying processes may often reveal new evidence as to the accuracy of the models. The present work attempts to examine numerically a turbulent, non-premixed, natural gas flame with and without consideration of the radiation effects. Two radiation models, namely the six-flux model and the discrete transfer model, have been used for this purpose.

The results have confirmed that the effect of thermal radiation is important on flame temperature predictions. The inclusion of radiative heat transfer in the combustion analysis has produced a better agreement between numerical predictions and experimental data. It has resulted to an increase of the levels of computed temperatures near the reactants inlet, and to a substantial decrease in the main combustion zone, near the walls, and the exit of the furnace. These observations indicate that the computations involving only convective heat transfer mechanisms under-predict the heating effect of the reactants mixture at the inlet, and over-predict the temperature levels everywhere else.

The inclusion of thermal radiation in the problem has also reduced the size of the flame region where maximum temperatures are located. Finally, it has increased about four times the percentage of heat leaving through the axial wall of the system, emphasizing the significance of this particular sink term in the total enthalpy balance analysis.

Finally, the two models have performed similarly, both showing good agreement with the experimental data. This indicates that the modeler can take advantage of the simplicity and low computational require-

ments of the six-flux model and use it with relative ease and confidence for describing the radiative heat transfer in natural gas-fired furnaces. Moreover, the discrete transfer model, although has shown a satisfying predictive accuracy that is not sensitive to optical properties and flame size, possesses some important disadvantages that the modeler should be aware of: (a) it is not as easy to incorporate into furnace codes, because it requires its own geometrical description, (b) it may prove tricky in terms of dividing the domain into zones to describe the geometry, and (c) is computationally more expensive.

References

[1] H. Guo, Y. Ju, K. Maura, T. Niioka, Radiation extinction limit of counterflow premixed lean methane–air flames, Combust. Flame 109 (1997) 639–646.

[2] A. Abbud-Madrid, D.P. Ronney, Effects of radiative and diffusive transport processes on premixed flames near flammability limits, in: Proceedings of the Twenty-Third Symposium (Int.) on Combustion, The Combustion Institute, Pittsburgh, 1990, pp. 423–431.

[3] S.H. Chan, X.C. Pan, M.M.M. Abou-Ellail, Flamelet structure of radiating CH_4–air flames, Combust. Flame 102 (1995) 438–446.

[4] A.S. Jamaluddin, P.J. Smith, Predicting radiative transfer in axisymmetric cylindrical enclosures using the discrete ordinates method, Combust. Sci. Technol. 62 (1988) 173–186.

[5] N. Selcuk, Evaluation for radiative transfer in rectangular furnaces, Int. J. Heat Mass Transfer 31 (1988) 1477–1482.

[6] F.C. Lockwood, N.G. Shah, A new radiation solution method for incorporation in general combustion prediction procedures, in: Proceedings of the Eighteenth Symposium (Int.) on Combustion, The Combustion Institute, Pittsburgh, 1981, pp. 1405–1416.

[7] A.C. Ratzell, J.R. Howell, Two-dimensional radiation in absorbing-emitting media using the P–N approximation, ASME J. Heat Transfer 105 (1983) 333–340.

[8] R.G. Siddall, Flux methods for the analysis of radiant heat transfer, J. Inst. Fuel 101 (1974) 101–109.

[9] N. Selcuk, N. Kayakol, Evaluation of discrete ordinates method for radiative transfer in rectangular furnaces, Int. J. Heat Mass Transfer 40 (1997) 213–222.

[10] F. Liu, H.A. Becker, Y. Bindar, A comparative study of radiative heat transfer modelling in gas-fired furnaces using the simple grey gas and the weighted-sum-of-grey-gases models, Int. J. Heat Mass Transfer 41 (1998) 3357–3371.

[11] S.R. Varnas, J.S. Truelove, Simulating radiative transfer in flash smelting furnaces, Appl. Math. Modelling 19 (1995) 456–464.

[12] H.C. Hottel, A.F. Sarofim, The effect of gas flow patterns on radiative transfer in cylindrical furnaces, Int. J. Heat Mass Transfer 8 (1965) 1153–1169.

[13] F.R. Steward, P. Cannon, The calculation of radiative heat flux in a cylindrical furnace using the Monte Carlo method, Int. J. Heat Mass Transfer 14 (1971) 245–262.

[14] L.D. Smoot, Pulverized coal diffusion flames: a perspective through modeling, in: Proceedings of the Eighteenth Symposium (Int.) on Combustion, The Combustion Institute, Pittsburgh, 1981, pp. 1185–1202.

[15] N. Hoffmann, N.C. Markatos, Thermal radiation effects on fires in enclosures, Appl. Math. Modelling 12 (1988) 129–140.

[16] N.S. Wilkes, P.W. Guilbert, C.M. Shepherd, S. Simcox, The application of HARWELL-FLOW3D to combustion models, AERE-R13508, in: Atomic Energy Authority Report, Harwell, UK, 1989.

[17] J.S. Truelove, Evaluation of a multi-flux model for radiative heat transfer in cylindrical furnaces, AERE-R9100, in: Atomic Energy Authority Report, Harwell, UK, 1978.

[18] N.C. Markatos, G. Cox, Hydrodynamics and heat transfer in enclosures containing a fire source, Physicochemical Hydrodynamics 5 (1984) 53–65.

[19] B.E. Launder, D.B. Spalding, The numerical computation of turbulent flows, Comp. Meth. Appl. Mech. Eng. 3 (1974) 269–283.

[20] B.F. Magnussen, B.H. Hjertager, On the mathematical modeling of turbulent combustion with special emphasis on soot formation and combustion, in: Proceedings of the Sixteenth Symposium (Int.) on Combustion, The Combustion Institute, Pittsburgh, 1976, pp. 719–730.

[21] E.P. Keramida, A.N. Karayannis, A.G. Boudouvis, N.C. Markatos, Radiative heat transfer in fire modeling, in: BFRL–NIST Annual Conference on Fire Research, NISTIR 6242, Gaithersburg, USA, 1998, pp. 147–149.